

Kinetics of zinc recovery from enyigba sphalerite in a binary solution of acetic acid and sodium nitrate

Ikechukwu A. Nnanwube¹, Judith N. Udejaja², Okechukwu D. Onukwuli³

¹Madonna University, Chemical Engineering Department, Faculty of Engineering, Akpugo, Enugu, Nigeria

²Nnamdi Azikiwe University, Chemical Engineering Department, Faculty of Engineering, Awka, Anambra, Nigeria

³Nnamdi Azikiwe University, Chemical Engineering Department, Faculty of Engineering, Awka, Anambra, Nigeria

Correspondence Author: Ikechukwu Abuchi Nnanwube, Madonna University, Department of Chemical Engineering, Faculty of Engineering, Akpugo, Enugu, Nigeria

Email: ik.nnanwube@gmail.com

Received date: 22 February 2020, Accepted date: 25 April 2020, Online date: 25 May 2020

Copyright: © 2020 Ikechukwu Abuchi Nnanwube et al, This is an open-access article distributed under the terms of the Creative Commons Attribution License, which permits unrestricted use, distribution, and reproduction in any medium, provided the original author and source are credited.

Abstract

Low-temperature hydrometallurgical leaching process has been identified as a viable route for recovering metals from their ores. In this study, the physicochemical characterization and dissolution kinetics of zinc recovery from sphalerite obtained from Enyigba in a binary solution of acetic acid and sodium nitrate was carried out. The physicochemical characterization of the ore was carried out using X-ray fluorescence; X-ray diffraction; Scanning electron micrograph, and Fourier transform infrared. The results show that the ore exists largely as zinc sulphide. The results showed that about 92.4% of sphalerite dissolved at the optimum conditions. The values of activation energy, reaction order, Arrhenius constant, and reaction constant were estimated as 34.603 kJ/mol, 0.706, 430.953 s⁻¹, and 2.22×10^6 s⁻¹, respectively. The kinetic data analysis showed that the experimental data followed the diffusion-controlled equation of the shrinking core model with chemical reaction as the rate-controlling mechanism. Hence, a binary solution of acetic acid and sodium nitrate has proved to be a viable means of recovering zinc from sphalerite.

Keywords: Sphalerite, Kinetics, Sodium Nitrate, Zinc, Leaching

INTRODUCTION

As the worldwide high grade ore reserves continue to deplete, hydrometallurgical route has provided an alternative to pyrometallurgical processes for sulphide ores and concentrates, principally for small scale production and for remote metal resources not suitable by pyrometallurgy (Rotuska and Chmielewski, 2008). In addition, hydrometallurgical route averts the production of SO₂, a pollutant (Guler, 2016).

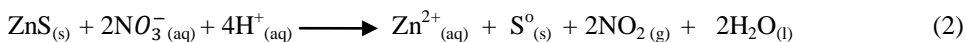
Sphalerite (ZnS) is the principal ore of zinc. About 95% of all primary zinc is extracted from sphalerite ores. However, owing to its variable trace element content, sphalerite is also an essential source of many minor metals, such as cadmium, germanium, and indium (Frenzel et al., 2017). Crystals of appropriate size and lucidity have been used to make gemstones, typically featuring the brilliant cut that demonstrate sphalerite's high dispersion-over three times that of diamond (Nnanwube, 2019).

Zinc and its compounds are used in most commercial and industrial applications. It is most commonly used in galvanization to protect metals such as iron and steel against corrosion. Zinc is the fourth most extensively used metal after iron, alumina, and copper. It is used as an alloying metal with copper to make brass, and as chemical compounds in rubber, ceramics, paints and agriculture. It is also an important element for adequate growth and development of humans, animals, and plant (Nwoye, 2013). Lorenzo-Tallafigo et al. (2018) reported on the kinetics of ferric leaching of sphalerite contained in a bulk concentrate. Two kinetic regimes, namely, the chemical reaction and the product layer diffusion controlled mechanisms were proposed for the study. The activation energy values of 51.3kJ/mol and 47.7kJ/mol were reported for the chemical reaction and diffusion through the non-porous film, respectively.

In acidic medium sphalerite releases zinc ion and forms elemental sulphur as illustrated in Equation (1).



Hence, the leaching of sphalerite in a binary solution of acetic acid and sodium nitrate is illustrated in Equation (2).



Leaching studies on the dissolution of sphalerite in acid solution have been reported. However, most of the reported studies focused on the application of inorganic acids such as hydrochloric acid (Baba and Adekola, 2010), nitric acid (Adebayo et al., 2006) and sulphuric acid (Hasani et al., 2016; Tian et al., 2018). There is no reported study-to the best of our knowledge-on the use of organic acid such as acetic acid as a lixiviant for sphalerite leaching. In the present study, the effectiveness of a binary solution of acetic acid and sodium nitrate as a lixiviant for zinc recovery from sphalerite has been investigated. The effects of process variables such as acetic acid concentration, sodium nitrate concentration, leaching temperature, stirring rate, solid/liquid ratio, and particle diameter on zinc recovery from Enyigba sphalerite was investigated. The kinetic analysis was carried out with the aid of the shrinking core model.

MATERIALS AND METHODS

Materials

The sphalerite sample obtained from Enyigba in south-eastern Nigeria was used. The sphalerite sample was crushed and sieved into five fractions: <75, 106-212, 212-300, 300-425, and >425 μm , using standard test sieves. The entire experiments were carried out with <75 μm fraction except otherwise stated. All chemicals used were of analytical grade and deionized water was used to prepare all solutions.

Methods

X-ray fluorescence spectroscopy (XRF) from X-supreme 60 oxford instruments was used to determine the chemical composition of the sphalerite sample. ARL X'TRA X-ray Diffractometer was used to carry out the mineralogical analysis of the ore sample using Cu K α radiation at 45kV and 40mA. The XRD patterns were recorded in the range of 5-65 $^\circ$ 2 θ . The surface morphology of the ore was analyzed using Scanning electron microscopy (SEM) Q250 by FEI model. The AAS analysis was conducted using Varian AA240 model.

The dissolution experiments were conducted in a 500 ml flat-bottomed flask. The glass was fixed to a condenser to avoid losses through evaporation. The calculated volumes of CH₃COOH and NaNO₃ solutions were added to the flask, which was then heated to a pre-set temperature with the aid of a magnetically-stirred hot plate. Subsequently, a sample with a pre-determined weight was added to the reactor. When the leaching time was completed, the materials that did not dissolve in the suspension was kept to settle and removed by filtration. The leach solutions were diluted and analyzed for zinc using atomic absorption spectrophotometer (AAS). Keeping other parameters constant, the influence of each parameter on the leaching rate was evaluated. (Onukwuli and Nnanwube, 2018).

Statistical analysis

The kinetic analysis was carried out with the aid of Microsoft Office Excel 2007 version.

RESULTS AND DISCUSSION

Characterization

The results of the X-ray fluorescence analysis of the sphalerite sample had earlier been reported (Onukwuli and Nnanwube, 2018). The result as shown in Fig. 1 revealed that ZnO, SO₃, Na₂O, and Fe₂O₃ were the major oxides present in the ore; oxides such as SiO₂, CaO, Al₂O₃, Mn₂O₃, and MgO were present in minor quantities while the rest occurred in traces.

The XRD result revealed the presence of sphalerite (ZnS) as the dominant mineral with three major peaks at 3.12, 1.91, and 1.63 \AA , respectively. The result also showed the presence of cerium germanium sulphide (Ce₂GeS₂) as an associated mineral with three major peaks at 2.96, 2.09, and 3.42 \AA , respectively (Onukwuli and Nnanwube, 2018).

The FTIR spectra of Enyigba sphalerite is shown in Fig. 2. The spectra shows the functional groups present in the ore. The band at 504.10 cm^{-1} is ascribed to C-N-C bend and C-O-C bend. The band at 839.08 cm^{-1} is attributed to C-Cl and Si-C stretches, while the band at 1066.67 cm^{-1} is ascribed to SO₃ symmetrical stretch as well as Si-O-Si anti-symmetrical stretch. The band at 1141.90 cm^{-1} is ascribed to C-C-N bending and C-O-C stretch, while the band at 1413.87 cm^{-1} is ascribed to C-N stretch and OH bending. The band at 1639.55 cm^{-1} is ascribed C=O and C=C stretches, while the band at 3396.70 cm^{-1} is ascribed to OH stretch.

The scanning electron micrograph (SEM) of sphalerite is presented in Fig. 3 with magnifications of 500x, 1000x, and 1500x, respectively. The results show that the particles exhibit uneven shapes and have rough edges. The particles also exhibited a high level of crystallinity.

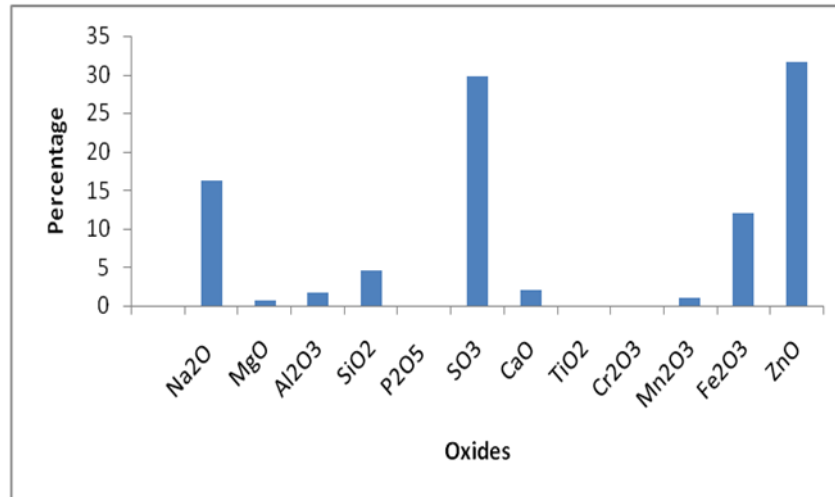


Figure 1: XRF result of Enyigba sphalerite

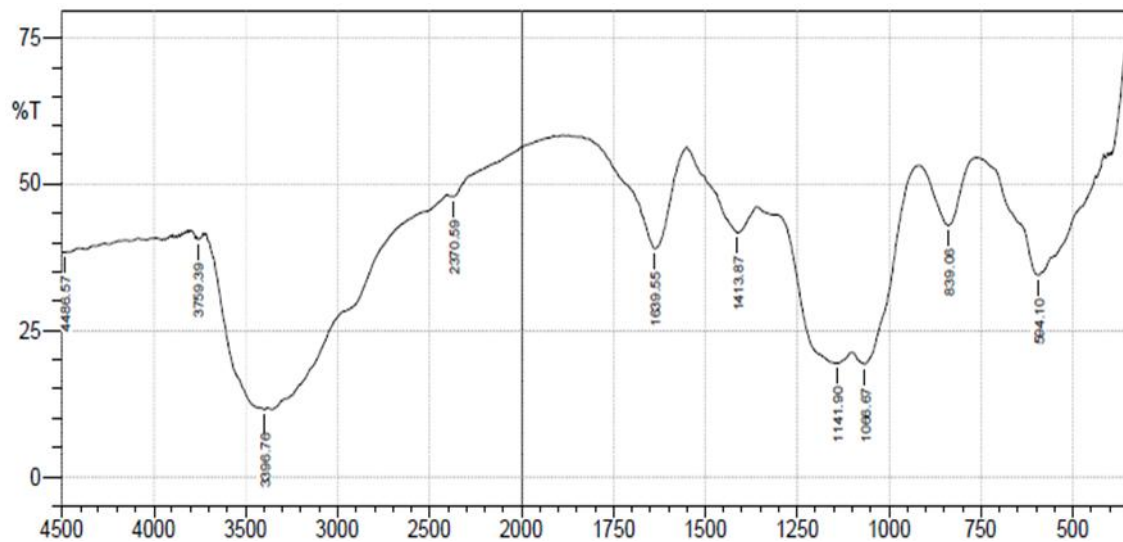


Figure 2: FTIR spectra of Enyigba sphalerite

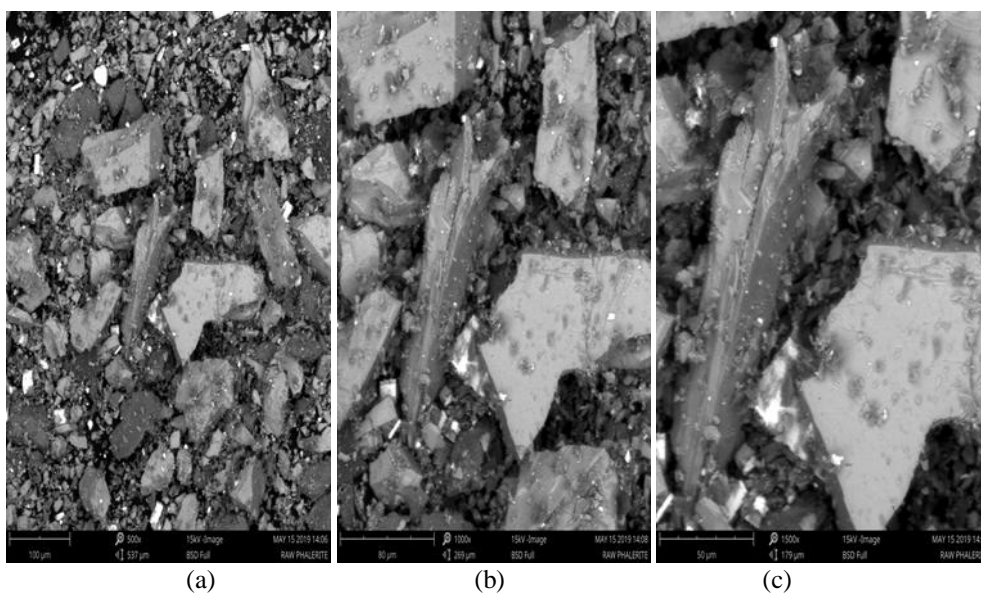


Figure 3: SEM images of sphalerite ore showing magnifications of 500× (a), 1000× (b), and 1500× (c), respectively

Effect of process variables on dissolution rate
Effect of NaNO₃ concentration in the presence of 0.1M CH₃COOH on sphalerite dissolution

To establish the influence of sodium nitrate concentration on zinc recovery from sphalerite, experiments were carried out with different values of NaNO_3 concentration. CH_3COOH concentration was kept constant at 0.1 M. A solid/liquid ratio of 20 g/L was used, while temperature and stirring rate were kept at 333K and 500 rpm, respectively. The results are shown in Fig. 4. From Fig. 4, it can be observed that the fraction of zinc recovered increased with the increase of sodium nitrate concentration. This is predominantly evident as the NaNO_3 concentration was increased from 0.2 to 0.6 M, after which no other increase in zinc recovery was recorded. This could be ascribed to a change in the rate determining step due to the considerable amount of elemental sulphur formed (Baba and Adekola, 2011). Hence, 0.6 M NaNO_3 was chosen as the optimum concentration and was used for other investigations.

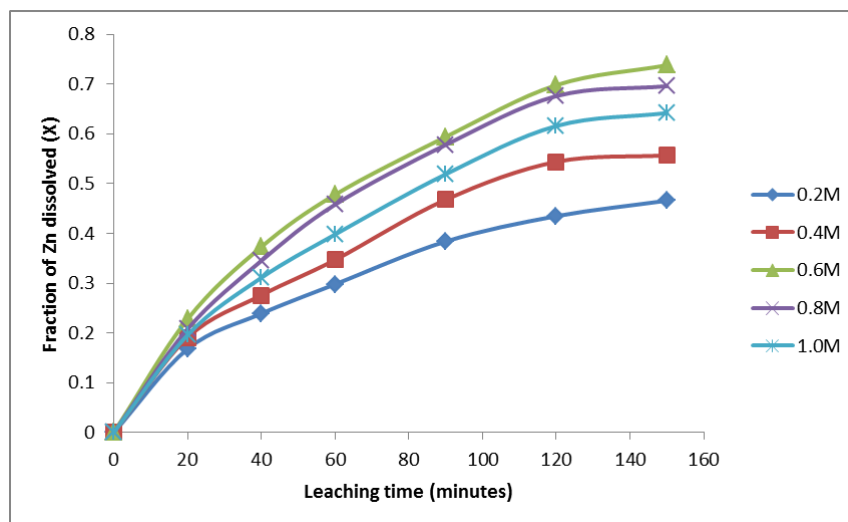


Figure 4: Effect of sodium nitrate concentration on sphalerite dissolution

Effect of varied CH_3COOH concentration in 0.6 M NaNO_3 on sphalerite dissolution

The effect of acetic acid concentration in 0.6 M NaNO_3 on the amount of zinc recovered was investigated at various CH_3COOH concentrations in the range of 2 – 12 M at 333K. Solid/liquid ratio and stirring rate were kept at 20 g/L and 500 rpm, respectively. The results as presented in Fig. 5 shows that the amount of zinc recovered increased with increase in acetic acid concentration and leaching time. The results obtained with 12 M CH_3COOH at 150 minutes leaching time (91.8 wt %) did not show any increase compared to that obtained with 10M CH_3COOH (91.9wt %), and this could be ascribed to the change in rate determining step at a higher reagent concentration due to the considerable amount of elemental sulphur formed (Baba and Adekola, 2018).

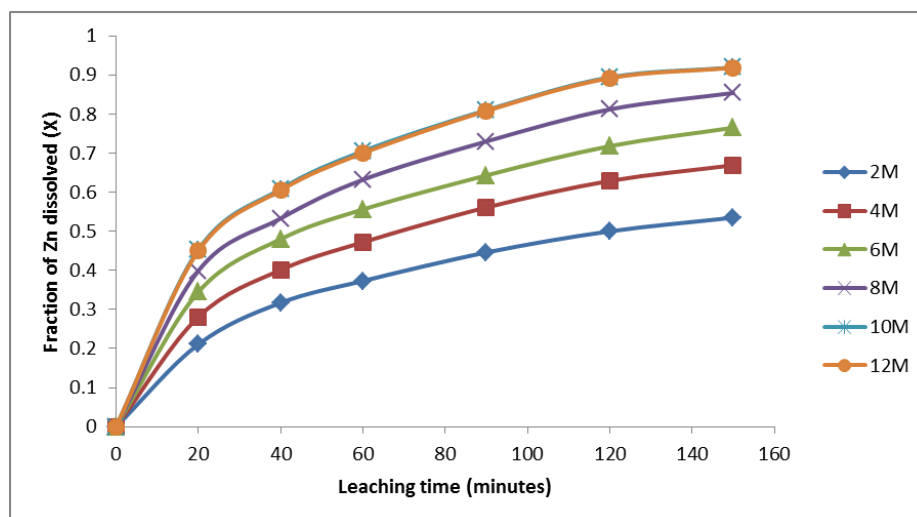


Figure 5: Effect of varied CH_3COOH concentration in the presence of 0.6M NaNO_3 on sphalerite dissolution

Effect of stirring rate

The influence of stirring rate on the recovery of zinc from sphalerite in 0.6 M NaNO_3 /10 M CH_3COOH is shown in Fig. 6. The solid/liquid ratio and temperature were kept constant at 20 g/L and 333K, respectively. The results show that the amount of zinc recovered increased with increase in stirring rate and leaching time. From the results shown in Fig. 6, the fraction of sphalerite dissolved was influenced by the stirring rate within the range 100-500 rpm. As the stirring rate was increased above 500 rpm, no appreciable increase was recorded on the amount of zinc recovered. About 91.9% zinc was recovered with NaNO_3 / CH_3COOH binary solution in 150 minutes.

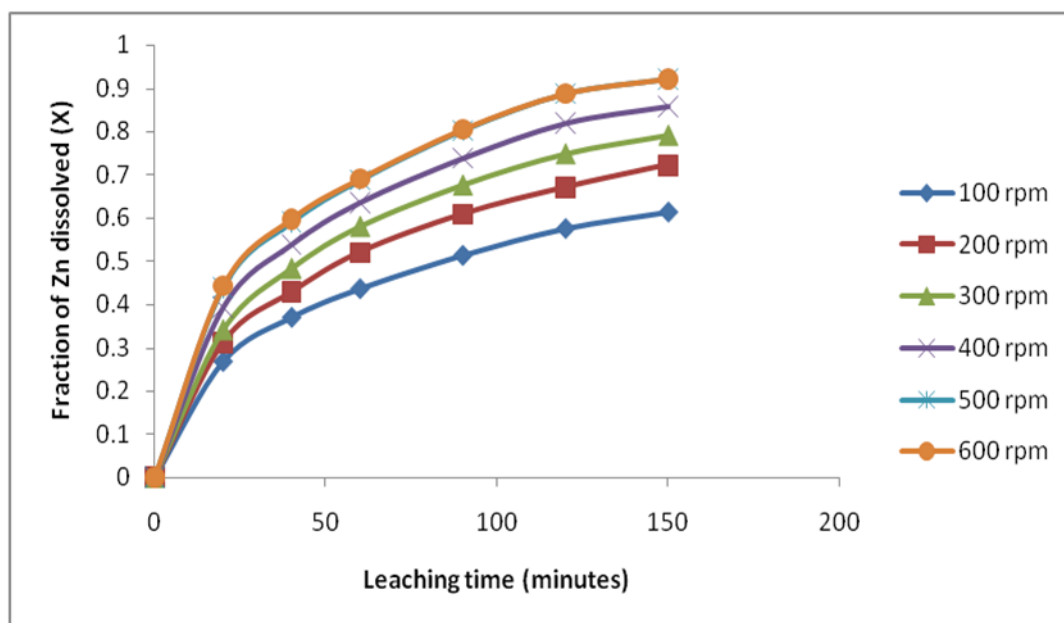


Figure 6: Effect of stirring rate on sphalerite dissolution

Effect of temperature

The influence of temperature on zinc recovery from sphalerite by 0.6 M NaNO_3 in the presence of 10 M CH_3COOH is shown in Fig. 7. Solid/liquid ratio and stirring rate were kept constant at 20 g/L and 500 rpm, respectively. The result revealed that the fraction of zinc recovered from sphalerite increased with increase in temperature and leaching time. With 0.6 M NaNO_3 in 10 M CH_3COOH about 92.4wt% of sphalerite dissolved within 150 minutes at 363K.

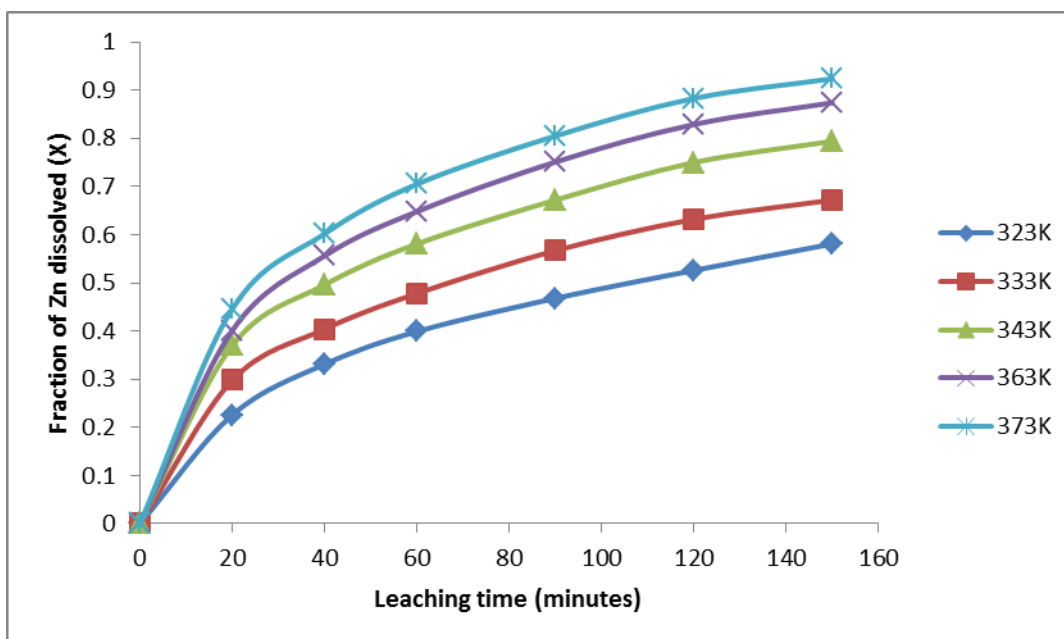


Figure 7: Effect of temperature on sphalerite dissolution

Effect of solid/liquid ratio on sphalerite dissolution

The influence of solid/liquid ratio on zinc recovery from sphalerite in 0.6 M NaNO_3 /10 M CH_3COOH were investigated within the range 0.02 to 0.045 g/ml as shown in Fig. 8. Stirring rate and temperature were kept at 500 rpm and 363K, respectively. The results show that the fraction of zinc recovered from sphalerite increased with decrease in solid/liquid ratio and increase in leaching time. About 92.5wt% zinc was recovered within 150 min at 363K in 0.6 M NaNO_3 /10 M CH_3COOH .

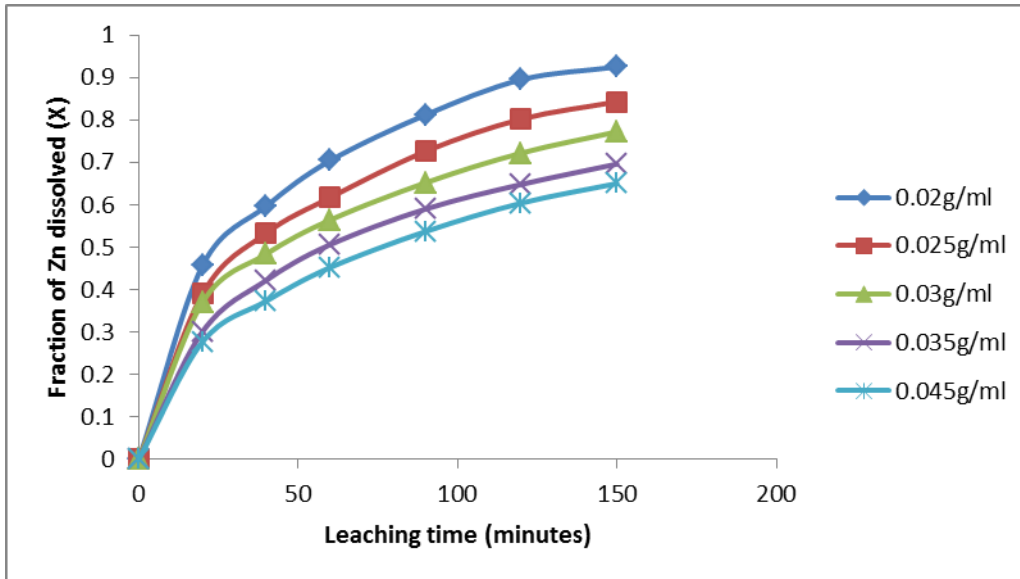


Figure 8: Effect of solid/liquid ratio on sphalerite dissolution

Effect of particle size

The effect of particle size on zinc recovery from sphalerite in 0.6 M NaNO_3 /10 M CH_3COOH was studied with five different particle sizes of the ore at 363K. Solid/liquid ratio was kept constant at 0.02 g/ml. The results as summarized in Fig. 9 show that the fraction of zinc recovered from sphalerite increased with increase in leaching time. The result showed that higher zinc recovery was recorded with smaller particle size. Similar result was also obtained by Aydogan et al. (2007a).

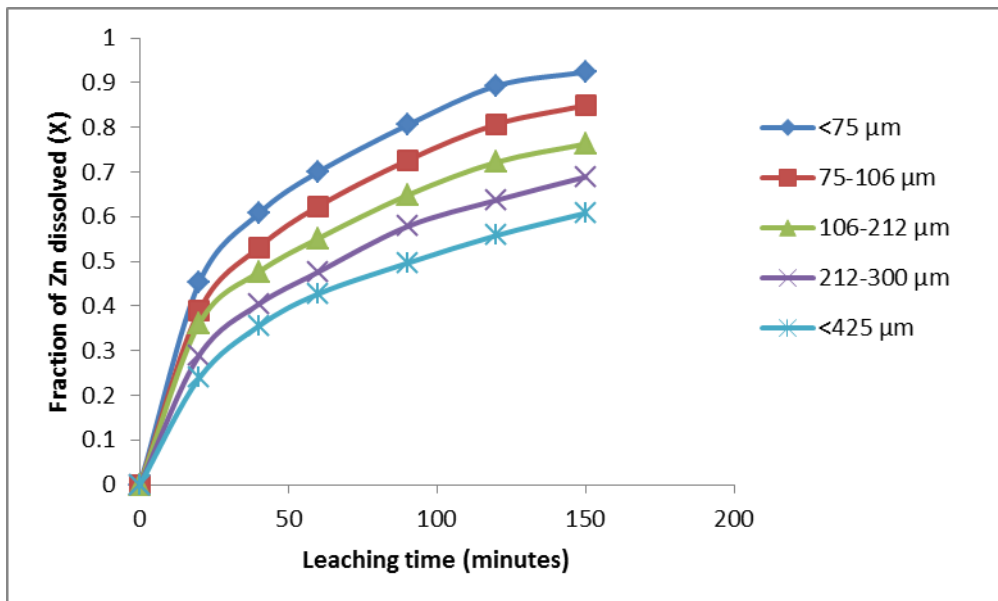


Figure 9: Effect of particle diameter on sphalerite dissolution

Dissolution Kinetic Models

To establish the kinetic parameters and rate-controlling step for the dissolution of sphalerite in $[\text{CH}_3\text{COOH}]_{0.6\text{M}} \text{NaNO}_3$ media, the experimental data plotted in Figures (5-9) were fitted to the shrinking core models as shown in Equations (3)-(6).

Equation (3) is for a chemical reaction controlled process at the interface. Equation (4) is applicable to a diffusion-controlled process through the product layer while Equation (5) is a mixed-controlled process (Onukwuli and Nnanwube, 2018).

$$1 - (1 - X)^{1/3} = \frac{bk_s C_A}{\rho_s r_o} t = k_2 t \quad (3)$$

$$1 + 2(1 - X) - 3(1 - X)^{2/3} = \frac{6bD_e C_A}{\rho_s r_o^2} t = k_3 t \quad (4)$$

$$1 - (1 - X)^{1/3} + (y/6) [(1 - X)^{1/3} + 1 - 2(1 - X)^{2/3}] = k_4 t \quad (5)$$

A modified form of the shrinking core model for product ash layer diffusion control as previously used by Baba and Adekola (2012) is shown in Equation (6).

$$1 - (2/3) X - (1 - X)^{2/3} = k_5 t \quad (6)$$

where X is the fraction reacted, k_5 is the kinetic constant, b is the stoichiometric coefficient of the reagent in the leaching reaction, C_A the concentration of the dissolved lixiviant, ρ_s the density of the solid, r_0 the initial radius of the solid particle, and D_e is the effective diffusion coefficient; k_2 is the rate constant from Equation (3) while k_3 , k_4 and k_5 are the rate constants for Equations (4), (5) and (6), respectively; y is assumed to be 1 for heterogeneous systems.

From the four models tested, the experimental data fitted into the relation in Equation (4), with higher correlation coefficients compared to other models. Hence, Figs. 5 – 9 were linearized using equation (4). From the data in Fig. 5, the model: $1 + 2(1 - X) - 3(1 - X)^{2/3} = k_1 t$, gave an average correlation coefficient of 0.995 as presented in Fig. 10.

A plot of $\ln K_1$ versus $\ln (\text{CH}_3\text{COOH})$ is shown in Fig. 13a and the slope of the plot indicates the order of the reaction with respect to acetic acid concentration. A value of 0.917 was obtained with a correlation coefficient of 0.987. The reaction order with respect to the stirring rate was obtained from the plot of the rate constants obtained by linearizing the data in Fig. 6 against $\ln w$ as shown in Figure 13b.

The results shown in Fig. 7 at various temperatures were linearized by Equation (4) and presented in Fig. 11. From the slopes of the lines in Fig. 11, the apparent rate constant, k_3 and other tested constants, k_2 , k_4 and k_5 were determined. The estimations of these rate constants with their proportional R^2 values are shown in Table 1.

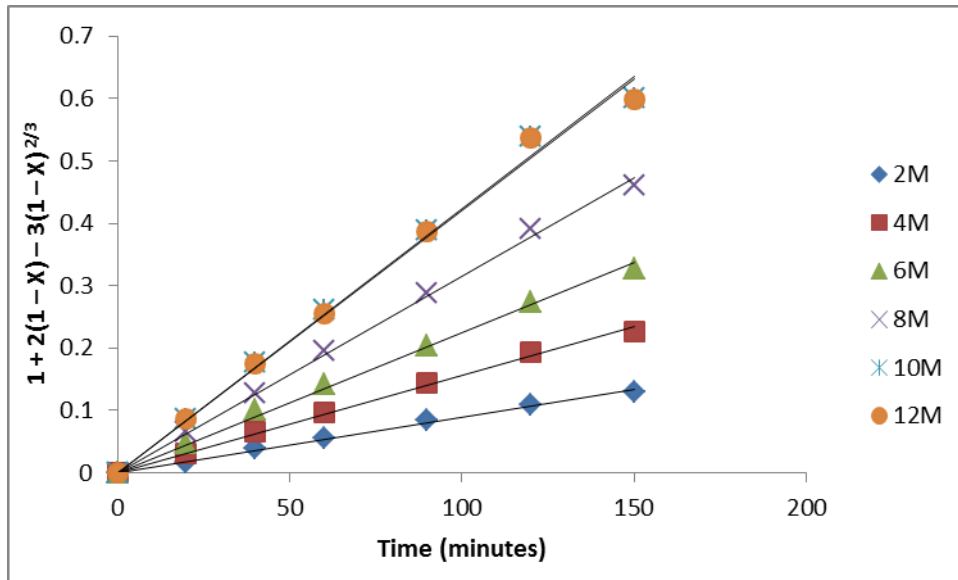


Figure 10: Plot of $1 + 2(1 - X) - 3(1 - X)^{2/3} = kt$ against leaching time at various CH_3COOH concentrations in the presence of 0.6 M NaNO_3 for data presented in Figure 5.

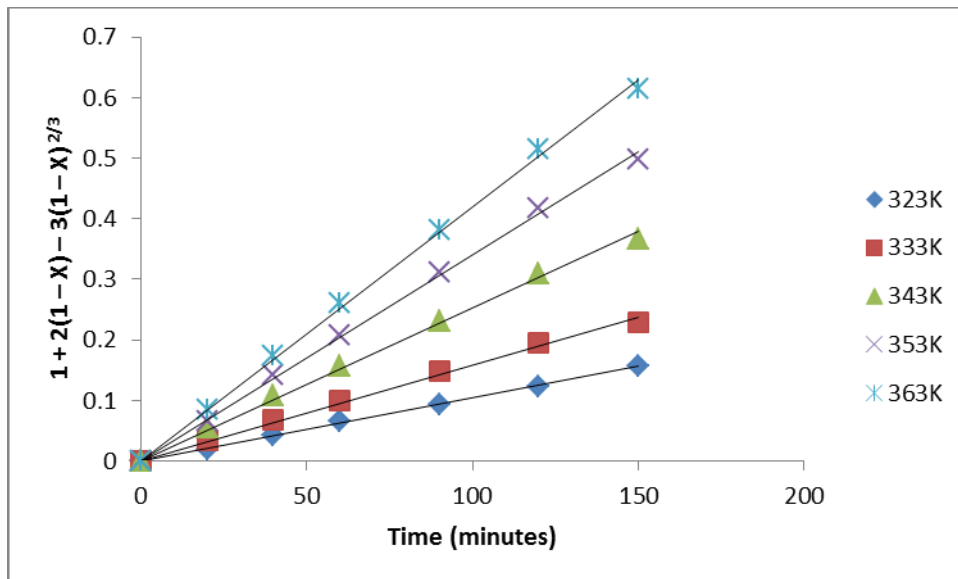


Figure 11: Plot of $1 + 2(1 - X) - 3(1 - X)^{2/3} = kt$ against leaching time at various temperatures for data presented in Figure 7

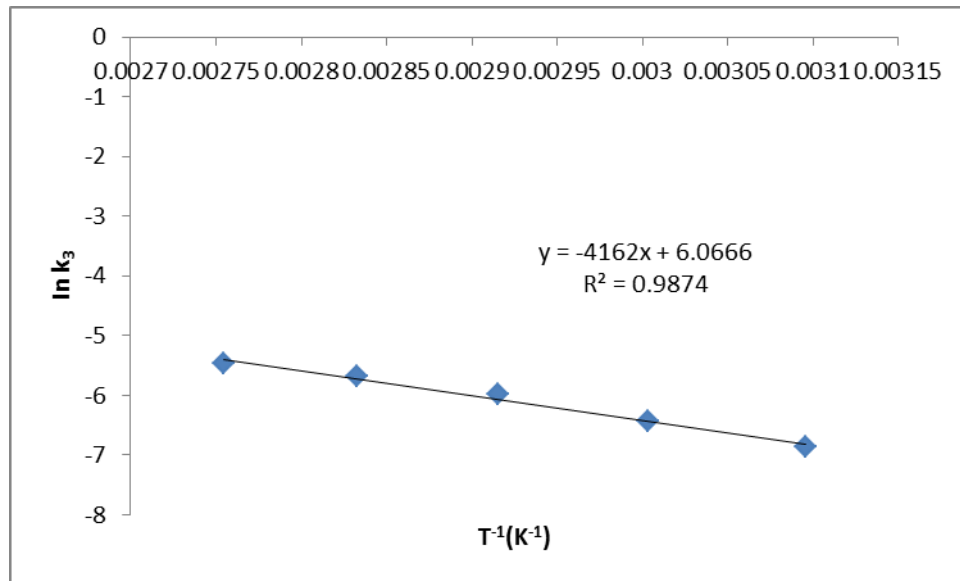


Figure 12: Arrhenius plot

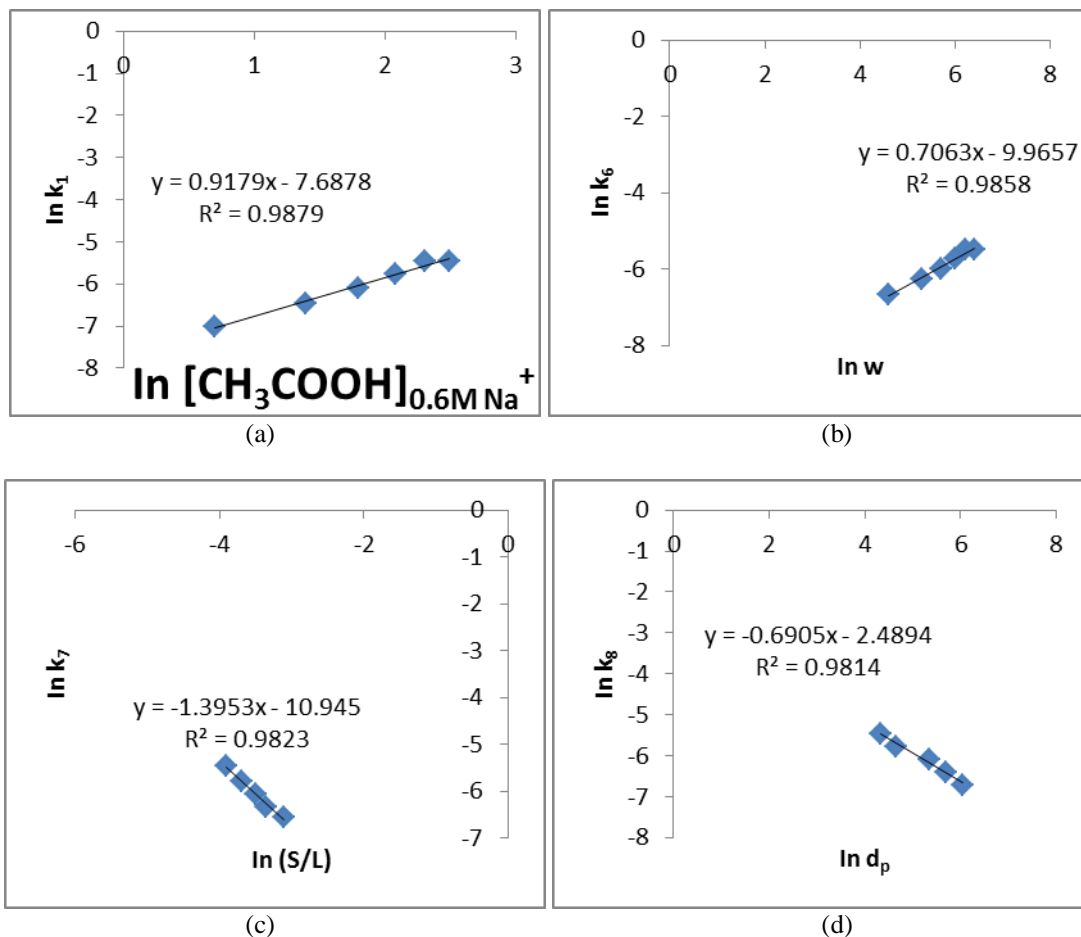


Figure 13: Plots to determine order of acid concentration (a), stirring rate (b), S/L ratio (c), and particle size (d)

Table 1: Values of the rate constants and regression coefficients (R^2) for sphalerite dissolution in 0.6M $NaNO_3$ /10 M CH_3COOH

Temperature (K)	Apparent rate constant ($\times 10^{-3}$) (min^{-1})				Correlation coefficient (r^2)			
	K_2	K_3	K_4	K_5	k_2	k_3	k_4	k_5
323	1.92	1.05	2.75	0.349	0.830	0.999	0.804	0.998
333	2.42	1.59	3.42	0.529	0.803	0.996	0.770	0.995
343	3.16	2.52	4.37	0.840	0.821	0.997	0.782	0.997
353	3.79	3.41	5.15	1.13	0.865	0.998	0.819	0.999
363	4.34	4.20	5.81	1.40	0.879	0.998	0.829	0.998

The temperature-dependence of the reaction rate constant is determined using the Arrhenius equation (Equation 7).

$$K_p = A \exp\left(\frac{-E_a}{RT}\right) \quad (7)$$

where A is the frequency factor, E_a is the activation energy, R is the universal gas constant, and T is the absolute temperature. A plot of $\ln K_p$ against $1/T$ gives a slope of E_a/R (Hasani et al., 2016). From the Arrhenius diagram shown in Fig. 12, the activation energy of 34.603 kJ/mol was obtained. The Arrhenius constant was also calculated, with a value of 430.953 s^{-1} . Hasani et al. (2016) had opined that activation energy of more than 30 kJ/mol indicates that a leaching process is controlled by a chemical reaction, while a value less than 30 kJ/mol is more likely to be controlled by diffusion through the product layer. However, other authors such as Babu et al. (2002) and (Baba and Adekola, 2012) obtained higher activation energy values for a diffusion-controlled process. From the results obtained in this study, the activation energy is higher than 30 kJ/mol, indicating a chemical reaction controlled process according to the postulation of Hasani et al. (2016). Hence, we conclude that the leaching of sphalerite in a binary solution of acetic acid and sodium nitrate is controlled by chemical reaction mechanism.

Dissolution Model

The apparent rate constants, K_7 and K_8 were evaluated from the linearized curves in Figs. (8 and 9). A plot of $\ln K_7$ versus $\ln[S/L]$ was plotted as shown in Fig. 13c, from which the reaction order with respect to the S/L ratio was obtained. The reaction order was found to be -1.359, with a slope proportional to $(S/L)^{-1.359}$. Similarly, a plot of $\ln K_8$ versus $\ln(d_p)$ is shown in Fig. 13d, from which a reaction order of -0.690 was obtained with respect to particle size, and with a slope proportional to $(d_p)^{-0.690}$.

From the activation energy obtained and the reaction orders with respect to the process parameters, the model for sphalerite dissolution in $\text{NaNO}_3/\text{CH}_3\text{COOH}$ binary solution at 363K is consistent with the equation below (Equation 8):

$$1 + 2(1 - X) - 3(1 - X)^{2/3} = k_o (\text{CH}_3\text{COOH})_{0.6\text{M NaNO}_3}^{0.706} (d_p)^{-0.690} (\rho \frac{S}{L})^{-1.395} (w)^{0.706} e^{(-34602.87/RT)} t.$$

(8) where ρ is the density of the ore. k_o is a reaction constant, evaluated from the fraction of sphalerite dissolved, X at any given time, t.

Characterization of the Residual Product

SEM Analysis of Sphalerite Leached with 10M $\text{CH}_3\text{COOH}/0.6\text{M NaNO}_3$

The morphology of sphalerite after leaching with 10M $\text{CH}_3\text{COOH}/0.6\text{M NaNO}_3$ binary solution by scanning electron micrograph (SEM) is presented in Fig. 14 with magnifications of 500 \times , 1000 \times and 1500 \times , respectively. The micrographs of the residues show an increase in the roughness of the particles. The particles have uneven shapes with rough edges and form microscopic flakes. The poor crystallinity of the particles may be due to attack by the lixiviant.

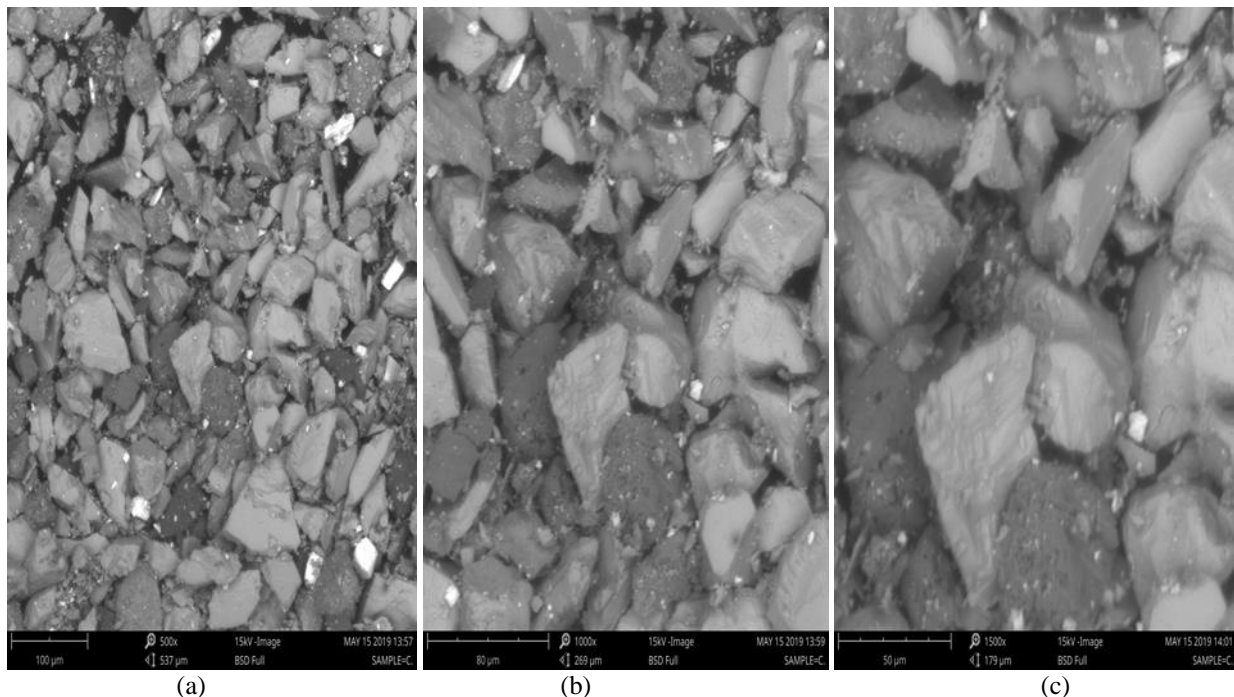


Figure 14: SEM image of sphalerite leached with 10M $\text{CH}_3\text{COOH}/0.6\text{M NaNO}_3$ with magnifications of 500 \times (a), 1000 \times (b), and 1500 \times (c), respectively

XRD Analysis of Sphalerite Leached with 10M $\text{CH}_3\text{COOH}/0.6\text{M NaNO}_3$

The analysis of sphalerite leached with 10M $\text{CH}_3\text{COOH}/0.6\text{M NaNO}_3$ at 363K by X-ray diffraction gives a description of the minerals found in the residue. Figure 15 present the results of the X-ray diffractogram of the residue which was recorded in the

range $5-75^\circ 2\theta$. The result revealed the presence of sphalerite (ZnS) with three principal peaks at 3.13, 1.91, and 1.63 Å, respectively, and galena (PbS) with three major peaks at 3.42, 2.97, and 2.10 Å, respectively, as shown in Fig. 15.

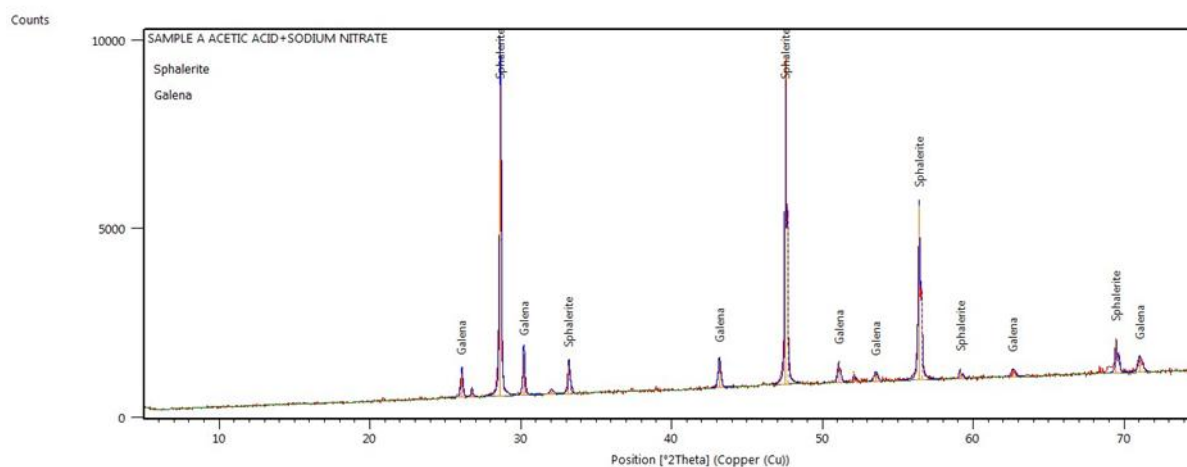


Figure 15: XRD pattern of sphalerite leached with $\text{CH}_3\text{COOH}/\text{NaNO}_3$

CONCLUSIONS

This study focused on the leaching kinetics of sphalerite in a binary solution of acetic acid and sodium nitrate. Characterization studies were carried out using X-ray fluorescence (XRF), X-ray diffraction (XRD), and scanning electron micrograph (SEM) and the results revealed that the ore exists mainly as zinc sulphide (ZnS). The result of kinetic studies showed that the experimental data followed the diffusion-controlled model, while chemical reaction model controlled the mechanism. Zinc recovery increased with increase in acetic acid concentration, temperature and stirring rate and decreased with increase in particle size and solid/liquid ratio. Analysis of the residue by XRD revealed the presence of sphalerite and galena.

CONFLICTS OF INTEREST

Authors declare no conflict of interest.

FUNDING STATEMENT

This research was not funded.

ACKNOWLEDGEMENT

The authors are grateful to the national research institute for chemical technology (NARICT), Zaria, Kaduna State, Nigeria, for performing the XRF, XRD, SEM and FTIR analyses.

AUTHORS' CONTRIBUTIONS

Dr. Ikechukwu Nnanwube contributed in the design of the experiment as well as in the statistical analysis of the work.

Judith Udejaja carried out the experimental aspects of the work.

Prof. Okechukwu Onukwuli contributed in the design of the experiment as well as in the theoretical aspects of the work.

REFERENCES

- Adebayo, A. O., K. O. Ipinmoroti, and O. O. Ajayi, 2006. Leaching of Sphalerite with Hydrogen Peroxide and Nitric Acid Solutions. *Journal of Minerals & Materials Characterization & Engineering*, 5(2): 167 – 177. <https://doi.org/10.4236/jmmce.2006.520126>.
- Aydogan, S., A. Aras and M. Cambazoglu, 2005. Dissolution Kinetics of Sphalerite in Acidic Ferric Chloride Leaching. *Chemical Engineering Journal*, 114: 67-72. <https://doi.org/10.1016/cej.2005.09.005>.
- Aydogan, S., M. Erdemoglu, G. Ucar and A. Aras, 2007. Kinetics of Galena Dissolution in Nitric Acid Solutions with Hydrogen Peroxide. *Hydrometallurgy*, 88: 52-57. <https://doi.org/10.1016/j.hydromet.2007.03.005>.
- Baba, A. A. and F. A. Adekola, 2010. Hydrometallurgical Processing of a Nigerian Sphalerite in Hydrochloric Acid: Characterization and Dissolution Kinetics. *Hydrometallurgy*, 101: 69 –75. <https://doi.org/10.1016/j.hydromet.2009.12.001>.

- Baba, A. A. and F. A. Adekola, 2011. Comparative Analysis of the Dissolution Kinetics of Galena in Binary Solutions of HCl/FeCl₃ and HCl/H₂O₂. *International Journal of Minerals, Metallurgy and Materials*, 18(1): 1-9.
- Baba, A. A. and F. A. Adekola, 2012. A Study of Dissolution Kinetics of a Nigerian Galena Ore in Hydrochloric Acid. *Journal of Saudi Chemical Society*, 16: 377 – 386. <https://doi.org/10.1016/j.jscs.2011.02.005>.
- Babu, M. N., K. K. Sahu and B. D. Pandey, 2002. Zinc Recovery from Sphalerite Concentrate by Direct Oxidative Leaching with Ammonium, Sodium and Potassium Persulphates. *Hydrometallurgy*, 64: 119 -129. [https://doi.org/10.1016/S0304-386X\(02\)00030-0](https://doi.org/10.1016/S0304-386X(02)00030-0).
- Frenzel, M., C. Mikolajczak, M. A. Reuter, and J. Gutzmer, 2017. Quantifying the Relative Availability of High-Tech By – product Metals - The Cases of Gallium, Germanium and Indium. *Resources Policy*. 52: 327-335. <https://doi.org/10.1016/j.resourpol.2017.04.008>.
- Guler, E., 2015. Pressure Acid Leaching of Sphalerite Concentrate: Modeling and Optimization by Response Surface Methodology. *Physicochemical Problems of Mineral Processing*, 52(1): 479-496. <https://doi.org/10.5277/ppmp160139>.
- Hasani, M., S. M. J. Koleini and A. Khodadadi, 2016. Kinetics of Sphalerite Leaching by Sodium Nitrate in Sulphuric Acid. *Journal of Mining and Environment*, 7(1): 1–12. <https://doi.org/10.22044/jme.2016.454>.
- Juan, L., I. Nieves, R. Rafael, M. Alfonso, and C. Francisco, 2018. Ferric Leaching of the Sphalerite Contained in a Bulk Concentrate: Kinetic Study, *Minerals Engineering*, 125: 50 – 59. <https://doi.org/10.1016/j.mineng.2018.05.026>.
- Nnanwube, I. A., 2019. Kinetics and Optimization Studies on the Hydrometallurgical Recovery of Zinc, Lead and Alumina from their Parent Matrices. PhD Thesis, Nnamdi Azikiwe University, Awka, Nigeria.
- Nwoye C. I., J. T. Nwabanne and J. U. Odo, 2013. Open System Leaching of Sphalerite in Butanoic Acid Solution and Empirical Analysis of Zinc Extraction Based on Initial Solution pH, Leaching Time and Mass-Input. *Research Journal of Chemical Sciences*, 3(5): 25-31.
- Onukwuli, O. D. and I. A. Nnanwube, 2018. Hydrometallurgical Processing of a Nigerian Sphalerite Ore in Nitric Acid: Characterization and Dissolution Kinetics. *The International Journal of Science and Technoledge*, 6(3): 40 -54.
- Rotuska, K. and T. Chmielewski, 2008. Growing Role of solvent Extraction in Copper Ores Processing. *Physicochemical Problems of Mineral Processing*, 42: 29-36.
- Tian, L., T. A. Zhang, Y. Liu, G. Z. Lv and J. J. Tang, 2018. Oxidative Acid Leaching of Mechanically Activated Sphalerite. *Canadian Metallurgical Quarterly*, 57(1): 59 – 69.